

---

# Counterfactual reasoning: an analysis of in-context emergence

---

Moritz Miller<sup>12</sup> \* Bernhard Schölkopf<sup>12</sup> Siyuan Guo<sup>13</sup>

<sup>1</sup>Max Planck Institute for Intelligent Systems <sup>2</sup>ETH Zurich <sup>3</sup>University of Cambridge

## Abstract

Large-scale neural language models (LMs) exhibit remarkable performance in in-context learning: the ability to learn and reason the input context on the fly without parameter update. This work studies in-context counterfactual reasoning in language models, that is, to predict the consequences of changes under hypothetical scenarios. We focus on studying a well-defined synthetic setup: a linear regression task that requires noise abduction, where accurate prediction is based on inferring and copying the contextual noise from factual observations. We show that language models are capable of counterfactual reasoning in this controlled setup and provide insights that counterfactual reasoning for a broad class of functions can be reduced to a transformation on in-context observations; we find self-attention, model depth, and data diversity in pre-training drive performance in Transformers. More interestingly, our findings extend beyond regression tasks and show that Transformers can perform noise abduction on sequential data, providing preliminary evidence on the potential for counterfactual story generation. Our code is available here.

## 1 Introduction

Thinking is acting in an imagined space. – Konrad Lorenz [Lorenz, 1973]

Large language models demonstrate remarkable capability in task-agnostic, few-shot performance, such as in-context learning and algorithmic reasoning [Brown et al., 2020]. Despite their success, one of the grand challenges of artificial general intelligence remains the ability to unearth novel knowledge. This requires principled reasoning over factual observations instead of inventing information when uncertain, a phenomenon termed hallucination [Achiam et al., 2023].

Thinking, in Konrad Lorenz’s words, is acting in an imagined space. Counterfactual imagination/reasoning, studied in early childhood cognition development [Southgate and Vernetti, 2014] and formalized in causality [Schölkopf, 2022, Pearl, 2009, Hernan, 2024], predicts the consequences of changes in hypothetical scenarios. It answers “what if” questions and predicts potential outcomes that could have occurred had different actions been taken. Such principled thinking enables *fast* and *responsible* learning, e.g., efficient reinforcement learning [Mesnard et al., 2021, Lu et al., 2020], counterfactual generative networks [Sauer and Geiger, 2021], responsible decision-making in complex systems [Wachter et al., 2017], and fairness [Kusner et al., 2017]. An exemplar reasoning statement reads, “John caught the flu at a gathering two nights ago and is recovering in bed. Had he not attended the get-together, he would now visit his grandmother for cake.” To perform counterfactual imagination, a reasoner acknowledges John’s present condition, formulates an imagined space in which John was not suffering from the flu, and acts therein: the reasoner infers that John would be visiting his grandmother. In precision healthcare, one may ask what would have happened *had a patient not received treatment* to assess the individualized treatment effect. Similarly, in language generation, an ideal model should be able to envision logically consistent theories for

---

\*Correspondence to moritz.miller@tuebingen.mpg.de

factual observation. Augmented with agentic verification, such principled counterfactual reasoning would be a valuable tool for automatic scientific discovery and a guardrail for safe AI deployment.

To concretely understand to what extent language models perform in-context counterfactual reasoning, we use the counterfactual framework of Pearl [2009] and study a controlled synthetic setup similar to Garg et al. [2022]. That is, let  $y = f(x, u_y)$  for some function  $f \in \mathcal{F}$ , for function class  $\mathcal{F}$ . The model predicts target  $y^{\text{CF}}$  given counterfactual query  $x^{\text{CF}}$  conditioned on a prompt sequence  $(x_1, y_1, \dots, x_k, y_k, z, x^{\text{CF}})$  where  $z$  is an index token indicating the position of the factual observation that such counterfactual query is based on. Given factual observation  $(x, y)$ , counterfactual reasoning requires three steps:

- noise abduction: infer  $u_y$  that is consistent with the factual observation  $(x, y)$ ,
- intervention  $do(X = x^{\text{CF}})$ : intervene on  $X$  to consider the hypothetical value  $x^{\text{CF}}$ ,
- prediction  $y^{\text{CF}} = f(x^{\text{CF}}, u_y)$ : predict the effect of changes  $x^{\text{CF}}$  in the context  $u_y$  inherited from the factual observation.

For a complete introduction on the basics of causality, see Section 2.1. In contrast to natural language, under this controlled setup, we can formally ask

*Can language models perform in-context counterfactual reasoning?*

with concrete metrics  $\mathbb{E} [\ell(y^{\text{CF}}, y_{\text{pred}}^{\text{CF}})]$ , for model prediction  $y_{\text{pred}}^{\text{CF}}$  and squared error function  $\ell$ .

This work studies counterfactual reasoning in exchangeable data, as we note language models are pre-trained on a mixture of sequences coming from different distributions. The training dynamics allow random permutations over different input sequences, i.e., implicitly assume sequences are exchangeable (see Def. 1). De Finetti [1931] shows that any exchangeable sequence can be modeled as a mixture of conditionally i.i.d. sequences. In other words, there exists a latent variable  $\theta$  with probability measure  $\pi$  such that  $P(s_1, \dots, s_n) = \int \prod_{i=1}^n p(s_i | \theta) d\pi(\theta)$ , for  $s_i$  the  $i^{\text{th}}$  sequence. Pre-training thus amounts to learning mutual information  $\theta$  between sequences and their prior  $\pi(\theta)$ . At inference time, the model computes the *posterior predictive distribution*: given a sequence  $s_i$  with tokens  $x_1^i, \dots, x_t^i$ , the next token prediction writes  $p(x_{t+1}^i | x_{\leq t}^i) = \int_{\theta} p(x_{t+1}^i | x_{\leq t}^i, \theta) \pi(\theta | x_{\leq t}^i) d\theta$ .

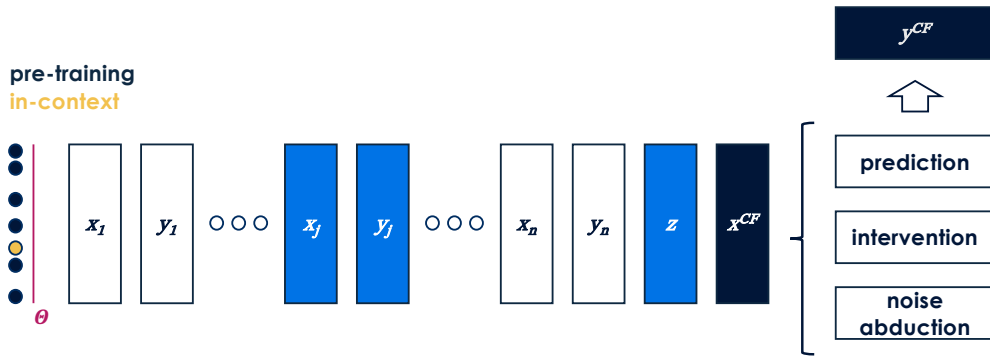


Figure 1: **In-context counterfactual reasoning.** Training on a corpus of sequences that come from a mixture of distributions (each  $\bullet$  on the far left represents a single sequence from a distinct distribution parameterized by  $\theta$ ). Suppose each observation satisfies  $y = f_{\theta}(x, u_y)$  for some noise  $u_y$ . An in-context sequence  $\bullet$  takes the form of  $n$  examples. This is concatenated with index token  $z$  referring back to observed factual observation  $(x_j, y_j)$  when  $z = j$  and the hypothetical new information  $x^{\text{CF}}$ :  $(x_1, y_1, \dots, x_n, y_n, z, x^{\text{CF}})$ . In-context counterfactual reasoning can be measured via accurate prediction on  $y^{\text{CF}}$ . Accurate prediction requires *noise abduction* from factual observation, that is, to infer  $u_y$  consistent with  $(x_j, y_j)$ , and *prediction* based on the *intervention*  $x^{\text{CF}}$  and inferred  $u_y$ .

Guo et al. [2024a,b] have established a theoretical foundation to study observational and interventional causality in exchangeable data. We extend this framework to counterfactuals. Building upon previous work, our contributions are:

- we provide insights into how in-context counterfactual reasoning is equivalent to transformations on in-context observations (Lemma 1).
- we empirically show that language models can perform in-context counterfactual reasoning (Section 4.1).
- we find that data diversity in pre-training, self-attention and model depth are key for Transformers’ performance (Section 4.2 and 4.3). More interestingly, our findings transfer to cyclic sequential data (Section 5), demonstrating concrete preliminary evidence that language models can perform counterfactual story generation in sequential data.

## 2 Background

### 2.1 Exchangeability and causality

**Definition 1** (Exchangeable sequence). A sequence of random variables is exchangeable if for any finite permutation  $\sigma$  of its indices,

$$\mathbb{P}(S_1, \dots, S_n) = \mathbb{P}(S_{\sigma(1)}, \dots, S_{\sigma(n)}).$$

Here we treat each random variable  $S_i$  as a sequence with bounded context length  $t$ .

**Causality fundamentals.** When  $X$  causes  $Y$ , the structural causal model (SCM) is determined by functional assignments  $f_X, f_Y$  and exogenous variables  $U_X, U_Y$ , i.e.,  $X := f_X(U_X), Y := f_Y(X, U_Y)$ . An intervention performed on variable  $X$  is represented as  $\text{do}(X = x)$ . Thus, one replaces  $X$  with value  $x$  and allows  $Y$  to inherit the replaced value, i.e.,  $X := x, Y := f_Y(x, U_Y)$ . A *counterfactual statement* of the form " $Y$  would be  $y$  had  $X$  been  $x$  in situation  $U = u$ " is often denoted as  $Y_x(u) = y$ . For explicit representation, we use  $y^{\text{CF}}, x^{\text{CF}}$  for values intended for counterfactual predictions. In contrast to the interventional setting, the counterfactual entity inherits context  $u_y$  consistent with the factual observation.

### 2.2 Transformer architecture

Transformers [Vaswani et al., 2017] operate on a sequence of input embeddings by passing them to blocks consisting of attention and a multi-layer perceptron (MLP). Mimicking present-day large language models, this work focuses on the decoder-only, autoregressive GPT-2 architecture for next token prediction. The softmax operation with causal masking is denoted by  $\text{softmax}_*$ . Given a sequence of input embeddings  $\mathbf{E} \in \mathbb{R}^{T \times E}$  of context length  $T$  and embedding dimension  $E$ , the model first projects each token into  $D$ -dimensional hidden embeddings via  $\mathbf{X}_0 = \mathbf{E}W_E + \text{pos}(\mathbf{E})W_P$ , for embedding matrix  $W_E \in \mathbb{R}^{E \times D}$ , positional embedding  $W_P \in \mathbb{R}^{T \times D}$  with absolute positional encoding. Given an input sequence of embeddings, multi-head attention at layer  $l$  passes the embeddings to query, key, value weight matrices  $W_Q^h, W_K^h, W_V^h \in \mathbb{R}^{D \times D}$  and computes attention per head as  $\mathbf{A}_l^h = \text{softmax}_* \left( \mathbf{X}_{l-1} W_Q^h (\mathbf{X}_{l-1} W_K^h)^\top \right)$ . Then the model concatenates the multi-head output and transforms it via output weight matrix  $W_O \in \mathbb{R}^{H \cdot D \times D}$  as  $\mathbf{M}_l = \text{Concat}(\mathbf{A}_l^1, \dots, \mathbf{A}_l^H)W_O$ . The output is added into the residual stream as  $\mathbf{R}_l = \mathbf{X}_{l-1} + \mathbf{M}_l$  and passed to an MLP  $\mathbf{X}_l = \text{MLP}(\mathbf{R}_l) + \mathbf{R}_l$ . After the last Transformer layer, the embeddings are mapped back to logits through the unembedding matrix:  $\mathbf{O} = \mathbf{X}_L W_U$ . We ignore layer normalization.

## 3 In-context counterfactual reasoning

We study a linear regression task that requires noise abduction. The structural causal model (SCM) considered is  $f_X(U_X) := U_X, f_Y(X, U_Y) := \beta X + U_Y$ , where  $U_X, U_Y$  are independent exogenous variables. We are interested in accurate counterfactual prediction on  $y^{\text{CF}}$  given new information  $x^{\text{CF}}$  and factual observation  $(x, y) = (u_x, \beta u_x + u_y)$ , where  $y^{\text{CF}} = \beta x^{\text{CF}} + u_y$ .

**Pre-training sequence generation.** Our pre-training corpus consists of a mixture of sequences coming from different distributions that share the same causal structure but different functional

classes. To generate a single sequence, we randomly draw a latent variable  $\theta$  and parameterize both the regression coefficient  $\beta$  and noise variables  $U_X, U_Y$  based on  $\theta$ . Each sequence takes the form  $(x_1, y_1, \dots, x_{n_i}, y_{n_i}, z, x^{\text{CF}}, y^{\text{CF}})$ , where  $n_i$  in-context examples are sampled from the SCM parameterized via  $\theta$  and  $z$  denotes the index token for that factual observation which the counterfactual query would be based on. We vary the number of in-context examples  $n_i$  observed at each sequence to avoid prediction based on information from positional encoding only. In particular, we respect the causal attention mask by ordering observed variables in topological order in a sequence format.

**Training objective.** We minimize  $\mathbb{E} [\ell(y^{\text{CF}}, y_{\text{pred}}^{\text{CF}})]$ , for  $y_{\text{pred}}^{\text{CF}}$  the model’s predicted outputs and  $y^{\text{CF}}$  the true counterfactual completion. We choose  $\ell$  to be the mean squared error (MSE).

In-context counterfactual reasoning can be represented via the posterior predictive distribution:

$$p(y^{\text{CF}} | x_1, y_1, \dots, x_n, y_n, z, x^{\text{CF}}) = \int_{\Theta} \int_{\mathcal{B}} \delta(Y^{\text{CF}} = \beta x^{\text{CF}} + y_z - \beta x_z) p_{\beta}(\beta | \mathbf{x}, \theta) \pi(\theta | \mathbf{x}) d\beta d\theta. \quad (1)$$

The model is required to learn how to compute posteriors  $p_{\beta}, \pi$  given a query at pre-training. In-context completion reduces to identifying  $z$ , inserting query elements  $(x_z, y_z, x^{\text{CF}})$  and weighting the resulting  $y_z^{\text{CF}}$  with the posterior of  $\beta$  given  $\mathbf{x}$ .

We first present Lemma 1 and show how accurate prediction on counterfactual values  $y^{\text{CF}}$  can be reduced to a transformation on in-context observations. Lemma 1 incorporates a broad class of functions, including additive noise models (ANMs) [Peters et al., 2011, 2014], multiplicative noise models and exponential noise models.

**Lemma 1** (Counterfactual reasoning as transformation on observed values). Suppose  $y = T(f(x), u)$  for some function  $T : \mathcal{F} \times \mathcal{U} \rightarrow \mathcal{Y}$ . Assume for any fixed  $f(x) \in \mathcal{F}$ , the inverse  $T^{-1}(f(x), \cdot)$  exists for all  $y$ , i.e.,  $u = T^{-1}(f(x), y)$ . Then, counterfactual reasoning reduces to learning a transformation  $h$  on observed factual observations  $(x, y)$  and counterfactual information  $x^{\text{CF}}$  with

$$y^{\text{CF}} = h(f(x), f(x^{\text{CF}}), y), \quad (2)$$

where  $h(f(x^{\text{CF}}), f(x), y) = T(f(x^{\text{CF}}), T^{-1}(f(x), y))$ .

Lemma 1 shows that given the existing information in the query, in-context counterfactual reasoning is no more than estimating the transformed function  $T, f, T^{-1}$  on the fly – a task Transformers are known to be capable of performing [Garg et al., 2022, Aky rek et al., 2023, von Oswald et al., 2023]. The assumptions in Lemma 1 cover a broad class of functions, for example,

- **Additive noise models (ANMs).** Functions taking the form  $Y = f(X) + U$  for arbitrary function  $f$  can be equivalently represented as  $y := T(f(x), u) = f(x) + u$ . For fixed  $f(x)$ , the inverse  $T^{-1}(f(x), \cdot)$  exists and reads  $u = T^{-1}(f(x), y) = y - f(x)$ .
- **Multiplicative noise models.** Functions taking the form  $Y = f(X) \cdot U$  for arbitrary function  $f$ . For fixed  $f(x)$ , the inverse  $T^{-1}$  exists and reads  $u = T^{-1}(f(x), y) = \frac{y}{f(x)}$ .
- **Exponential noise models.** Functions taking the form  $Y = \exp(f(X) + U)$  with inverse  $u = T^{-1}(f(x), y) = \log(y) - f(x)$ .

## 4 Experiments

Based on the training setup described in Section 3 with details in Appendix C, we choose a controlled synthetic setup to allow concrete evaluation on in-context counterfactual reasoning.

### 4.1 Language models can in-context perform counterfactual reasoning on linear functions

We assess the impact of model architecture choice on in-context counterfactual reasoning performance. In contrast to natural language tasks, the performance in our task is clearly defined and can be measured as:

- *accuracy* in prediction:  $\text{MSE}(y^{\text{CF}} - y_{\text{pred}}^{\text{CF}})$ ,

- *learning efficiency*: number of in-context examples seen to achieve satisfactory prediction.

We compare the STANDARD decoder-only GPT-2 Transformer architecture against several autoregressive baselines. We use the terms STANDARD and GPT-2 interchangeably. The models considered are:

- GPT-2 [Radford et al., 2019]: 12 layers, 8 attention heads, hidden dimension 256,
- LSTM [Hochreiter and Schmidhuber, 1997]: 3 layers, hidden dimension 256,
- GRU [Cho et al., 2014]: 3 layers, hidden dimension 256,
- ELMAN RNN [Elman, 1990]: 3 layers, hidden dimension 256.

We evaluate each model on unseen sequences sampled in-distribution and report results averaged over 100 sequences. Our synthetic generation yields  $\mathbb{E}[Y^{\text{CF}}] = 0$  and  $\log(\text{std}(Y^{\text{CF}})) = 2.56$ . Appendices C and D include data generation particularities as well as experimental and model details.

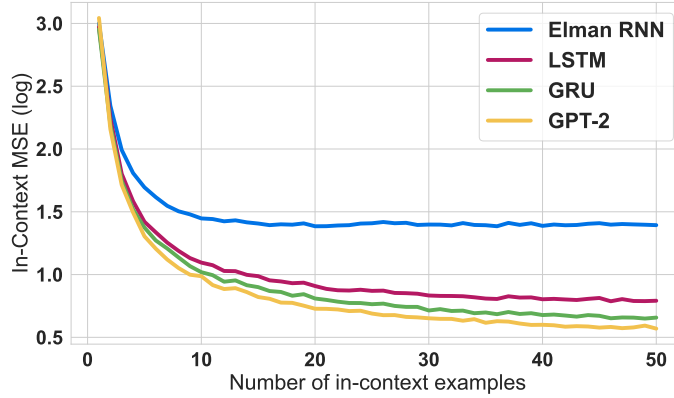


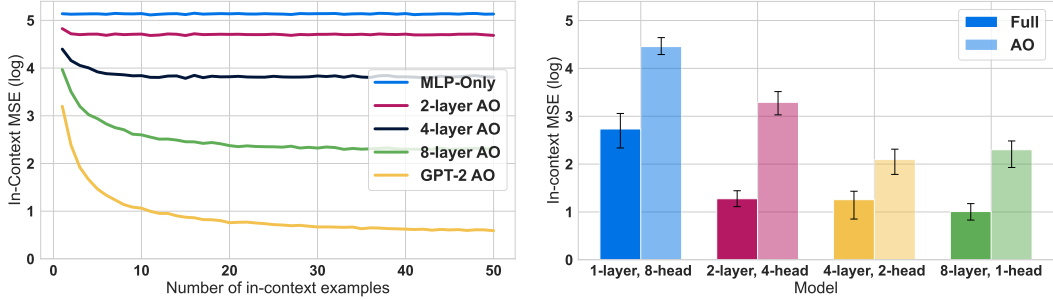
Figure 2: **Model comparisons for in-context counterfactual reasoning.** In-context counterfactual prediction accuracy measured via log-transformed mean-squared error loss averaged over 100 sequences versus the number of in-context examples observed in a prompt. We compare the following model architectures: GPT-2 (STANDARD), LSTM, GRU, and Elman RNN. All models are capable of in-context counterfactual reasoning. GPT-2 (STANDARD) achieves lowest error and fastest convergence rate for a small number of in-context examples.

Figure 2 compares the impact of different model architectures on in-context counterfactual reasoning. We plot the log-transformed in-context MSE against the number of in-context examples observed in a prompt. We hypothesize that more observed examples lead to higher counterfactual prediction accuracy, and that better models require less in-context examples for accurate prediction. Our result shows that all models achieve a loss within one standard deviation of the expected mean. With sufficient context, GPT-2 (STANDARD) scores the lowest MSE (near optimal). It also demonstrates the fastest convergence rate in in-context loss given a small number of in-context examples.

## 4.2 Counterfactual reasoning emerges in self-attention

**Self-attention.** Lemma 1 shows the reliance of counterfactual reasoning on copying in-context observed values. Self-attention has been shown to perform copying by implementing induction heads [Olsson et al., 2022, Akyürek et al., 2024]. We thus hypothesize that counterfactual reasoning emerges in the attention sublayers of the Transformer.

We conduct an experiment that switches on and off attention layers in the Transformer and separately train each model on our task. Figure 3a shows the in-context MSE loss for **MLP-Only** and **GPT-2 AO** (attention only) with 2, 4, 8 layers and the STANDARD setup. At training time, we observe that **AO** models mimic the loss curve of the STANDARD setup, while the **MLP-Only**’s loss remains constant at the level of the theoretical variance,  $\text{Var}(Y^{\text{CF}})$ . Figure 3a shows that counterfactual reasoning performance improves for all considered Transformers with increasing context length. Although at a higher loss than the STANDARD Transformer, smaller models do perform better on longer contexts. Oblivious of context length, **MLP-Only** does not appear to reason counterfactually.



(a) **Switching attention.** In-context MSE stagnates with increasing number of in-context examples observed for the **MLP-Only** model. We compare to attention-only (**AO**) Transformers of 2, 4, 8 layers and the STANDARD GPT-2 setup. For all Transformers, in-context MSE decreases as more in-context examples are observed.

(b) **Varying depth.** Keeping the number of attention heads constant at 8, we compare **Full** and **Attention Only (AO)** Transformers with 1 layer, 8 heads; 2 layers, 4 heads; 4 layers, 2 heads; 8 layers, 1 head. We observe a decrease in in-context loss as model depth increases. We evaluate on 100 sequences of 35 in-context examples.

Figure 3: **Attention and model depth matter.**

**Model Depth.** Elhage et al. [2021] show that self-attention performs a copying task. Lemma 1 relates counterfactual reasoning to copying multiple values and learning transformations. Such a task requires the composition of attention heads to pass information across layers. We hypothesize that model depth plays an important role. Fixing the total number of attention heads at 8, we train 4 Transformer-based models with increasing depth: from 1-layer, 8-head Transformers to models with 8 layers of 1 head each. We expect that if depth does not influence performance, given the same number of attention heads, all models should have comparable in-context MSE. Figure 3b represents the loss on 100 sequences of 35 in-context examples for both **Full** and **AO** models. Additional results can be found in appendix D. With increasing depth, loss declines for both setups. In particular, the **Full** 8-layer, 1-head Transformer yields lowest MSE, while the 4-layer, 2-head designs achieve competitive results.

### 4.3 Data diversity and out-of-distribution (OOD) generalization

Causal structure identification, a previously deemed impossible task from i.i.d. observational data alone [Pearl, 2009], has been shown to be feasible in multi-domain data [Guo et al., 2024a], a natural setting for exchangeable data. We hypothesize that (counterfactual) reasoning is similarly only feasible under diverse pre-training data. As a measure of pre-training data diversity, we use the effective support size [Grendar, 2006], defined as

$$\text{Ess}(\theta) := \exp \left( - \sum_{\vartheta \in \Theta_0} p(\vartheta) \log p(\vartheta) \right) = \exp(H(\theta)),$$

where  $\Theta_0$  is the space of latent  $\theta$  sampled in pre-training, and  $H$  the Shannon entropy [Shannon, 1948]. We further compare the pre-training data diversity’s impact on simple *OOD* generalization. We pre-train on both UNIFORM and NORMAL sampling of latent  $\theta$  and evaluate on UNIFORM sampled test data. Figure 4 shows a clear trend that diverse pre-training data, measured as a higher effective support size gives lower in-context MSE loss for both in-distribution and *OOD* cases. Appendix E shows that such generalization ability persists when evaluated on NORMAL, and that in-context loss declines with increasing data diversity across a changing number of in-context examples.

### 4.4 Beyond linear regression: robustness to non-linear, non-additive functions

To test Transformers’ in-context counterfactual reasoning performance beyond linear regression tasks, we pre-train models on different non-linear and non-additive functions satisfying the invertibility condition specified in Lemma 1. We generate data with function classes parameterized by tanh and  $\sigma$  activations as well as multiplicative noise separately. We observe that all three function classes lead to reduced squared error relative to the empirical variance of target  $Y^{\text{CF}}$ , suggesting Transformer’s in-

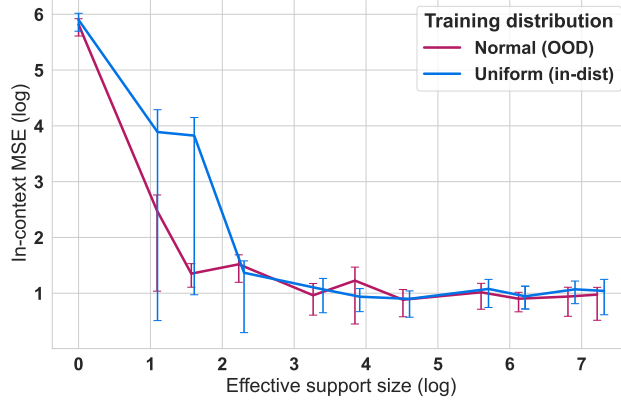


Figure 4: **Data diversity in pre-training.** We measure in-context MSE (log-scaled) averaged over 100 prompts at 35 in-context examples against log-scaled effective support size. Each point represents one fully pre-trained model on either the UNIFORM sampled or NORMAL sampled  $\theta$ . All models in this plot are evaluated on the UNIFORM dataset. Error bars are the 95% basic bootstrap confidence intervals [Efron, 1979]. We observe a clear trend that as data diversity increases, in-context counterfactual reasoning loss decreases.

context counterfactual reasoning ability is robust to different function classes beyond linear regression. Appendix E describes the detailed setup and results on the tested invertible activations.

## 5 Cyclic sequential dynamical systems

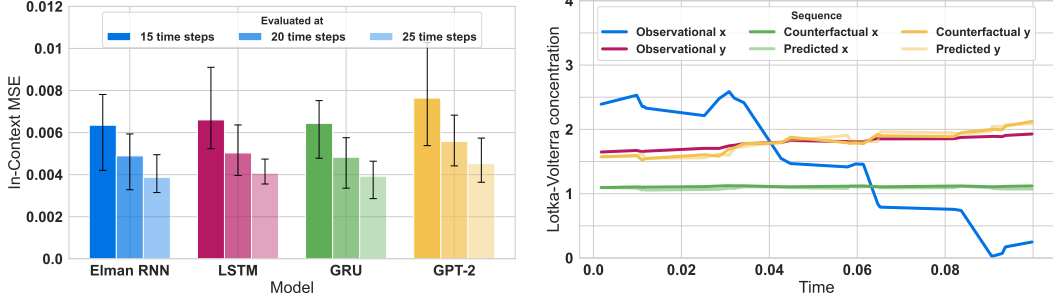
Language is sequential. Sentences within a story depend on each other. Counterfactual story generation naturally occurs by prompting the model with a factual story and querying it to complete the story under a hypothetical scenario. This is done while keeping the context unchanged. Although difficult to evaluate in language, our key insight is that such behavior can be mimicked by ordinary differential equations modeling the underlying causal mechanism [Mooij et al., 2013, Peters et al., 2022, Lorch et al., 2024]. Given an initial configuration  $(x_0, y_0)$ , a dynamical system determines the state  $(x_t, y_t)$ , for  $t \geq 0$ . We model causal dependencies using Itô stochastic differential equations (SDEs),

$$\begin{aligned}
 dY_t &:= f(X_t, Y_t)dt + \sigma_Y \cdot dW_t \\
 dX_t &:= g(X_t, Y_t)dt + \sigma_X \cdot dU_t \\
 X_0 &:= \xi_0 \text{ and } Y_0 := v_0,
 \end{aligned} \tag{3}$$

for initial configuration  $(\xi_0, v_0)$ . Here,  $W_t, U_t$  denote independent Brownian motions with constant diffusion by  $\sigma_X, \sigma_Y$ , and  $f, g$  represent the drift coefficients for  $X, Y$ , respectively.

Autoregressive models are discrete. To address the challenge of adapting continuous SDE data generation to discrete observations, we randomly select independent timestamps from the real line. In particular, we draw  $N$  event times from a Poisson point process on a bounded interval. We evaluate the above SDE at time  $t_n$  for all  $n \leq N$  and input observations to the model. Instead of deterministically slicing the interval into equivalent regions, we can capture the complete bounded interval as the randomly sampled set of event times, independent across iterations. Noise abduction is thus required over both the realization of  $u$  and of event times  $t_n \leq t_N$ .

In summary, we provide context  $(x_0, y_0, \dots, x_{t_N}, y_{t_N})$ , a counterfactual token indicating the start of counterfactual story generation, and an initial counterfactual configuration  $(x_0^{\text{CF}}, y_0^{\text{CF}})$ . Then, we train the model on completing the full counterfactual story. We thus ask the model to generate  $(x_{t_1}^{\text{CF}}, y_{t_1}^{\text{CF}}, \dots, x_{t_N}^{\text{CF}}, y_{t_N}^{\text{CF}})$ . Models are evaluated based on MSE across all predicted tokens. Contrary to above, we assess performance not just on the final token, but over the entire counterfactual continuation consisting of  $(N - 1) \cdot 2$  tokens. Additionally, the full context corresponds to a *single* instance of a factual story. Given this story, the model must infer the noise associated with all observational examples, rather than just a single example pair. We thus have deterministic functional



(a) **In-context evaluation on Lotka-Volterra SDEs.** In-context MSE of four models queried with data on 15, 20, and 25 distinct time points. Across models, MSE declines as context length increases. While STANDARD GPT-2 Transformer has highest MSE, basic bootstrap confidence intervals suggest that performance across models is competitive. (b) **Prediction of Lotka-Volterra SDEs in-context.** The query consists of the observational interwoven  $(x, y)$  data. In-context, the model learns the dynamics governed by the latent  $\theta$  and completes the counterfactual trajectory for all  $t_n > 0$ . Although observational  $x$  spans  $[0, 2.6]$ , the model infers that counterfactual  $x^{\text{CF}}$  is constrained to  $[1.05, 1.15]$ .

Figure 5: Cyclic causal relationship.

assignments  $f, g$ , and copy the noise  $W_t, U_t$  from the observational sequence. With constant diffusion, we invoke Lemma 1, which connects the cyclic extension to the regression setup,

$$Y_t^{\text{CF}} = \int_0^t f(X_s^{\text{CF}}, Y_s^{\text{CF}}) ds - \int_0^t f(X_s, Y_s) ds + Y_t. \quad (4)$$

We conduct preliminary experiments on data generated from the Lotka-Volterra model [Lotka, 1910] describing predator-prey dynamics,

$$g(X_t, Y_t) := \alpha X_t - \beta X_t Y_t \quad (5)$$

$$f(X_t, Y_t) := -\gamma Y_t + \delta X_t Y_t \quad (6)$$

with  $\alpha, \beta, \gamma, \delta \geq 0$ . Appendix F specifies training and data generation details and analyzes the attention behavior in the Transformer. Figure 5a shows that Elman RNNs obtain the lowest in-context MSE across the four studied models. Error bars [Efron, 1979] point to competitive performance across architectures. We evaluate the models on contexts of  $N = 15, 20, 25$  realizations of in-context pairs  $(x_{t_N}, y_{t_N})$ . Recall that these are not *conditionally i.i.d.* in-context examples as above, but rather follow a sequential pattern. Figure 5b illustrates this sequentiality. Given a query consisting of interleaved observations of the prey, predator concentrations  $(x, y)$ , the model infers the underlying latent  $\theta$  governing the system. It then infers the full counterfactual trajectory beyond the initial configuration. Notably, while the observed  $x$  values span a broad range  $[0, 2.6]$ , the model correctly infers that the counterfactual  $x^{\text{CF}}$  is confined to a narrow interval  $[1.05, 1.15]$ . This indicates that the model internalizes the underlying dynamics and uses them to generate coherent predictions.

## 6 Discussion and related work

**Counterfactual reasoning in Language.** This work is motivated by the study of in-context *counterfactual reasoning* in language models. For principled reasoning, it is important to enable automatic scientific knowledge discovery and to ensure safety in deployment. We start with an analysis of a simple case: given a pair of sentences  $(x_j, y_j)$ , where  $x_j$  is semantically ambiguous, and  $y_j$  resolves the ambiguity. Prompted on a sequence of conditionally independent examples, the language model has to concretize another ambiguous sentence under the setting of the  $z^{\text{th}}$  example. Thus, the model infers the semantic ambiguity from the in-context example  $(x_z, y_z)$  and completes the query accordingly. See a detailed example provided in Appendix G.

Preliminary investigation on *counterfactual story generation* has been mainly focused on empirical evaluation on off-the-shelf language models. Tandon et al. [2019], Li et al. [2023] study lexical associations between factual statements and the hypothetical "what if" scenario; Qin et al. [2019] provide a dataset for counterfactual rewriting evaluation. Bottou and Schölkopf [2025] link the ability



to hypothesize about counterfactuals to generating meaningful text beyond the training distribution. Ravfogel et al. [2025] study language directly as structural causal acyclic models and Yan et al. [2023] focus on representation identification for adaptive counterfactual generation. This work respects the sequential nature of language and performs controlled pre-training and concrete evaluations that demonstrate preliminary and promising evidence that language models are capable of counterfactual story generation.

**In-context learning.** Language models [Brown et al., 2020] have shown surprising in-context reasoning ability demonstrating the potential for practical user interactions in the form of chatbots. Transformers, the backbone architecture for modern language models, have been shown to in-context learn different function classes [Garg et al., 2022]. Some studies investigate the models’ ability to perform gradient descent over in-context examples [Dai et al., 2023, Deutch et al., 2024, von Oswald et al., 2023] while others discuss implicit Bayesian inference [Xie et al., 2022, Falck et al., 2024, Ye and Namkoong, 2024] and *induction heads* [Olsson et al., 2022, Akyürek et al., 2024]. A recent line of work considers guarantees for in-context learning algorithms on linear models [Akyürek et al., 2023].

**Causality and exchangeability.** Pearl [2009], Hernan [2024] formalize the notion of counterfactuals in causality. Peters et al. [2022], Lorch et al. [2024] study cyclic causal models via differential equations. Mixture of i.i.d. data or multi-domain data have been the foundation of modern pre-training corpora. Guo et al. [2024a] demonstrate that inferring causality is feasible in such a mixture of i.i.d. data, providing the potential for language models to exhibit causal reasoning capabilities. Recent work has continued to investigate connections between causality and exchangeability from intervention [Guo et al., 2024b] to representation learning [Reizinger et al., 2025]. Concurrently, interest in exchangeability and language models has resurfaced: Zhang et al. [2023] study topic recovery from language models and Falck et al. [2024], Ye and Namkoong [2024], Xie et al. [2022] discuss in-context learning as performing implicit Bayesian inference in the manner of de Finetti. This provides potential for *causal* de Finetti, which allows structured in-context learning with the potential for principled reasoning and fast inference. This work provides a preliminary study on counterfactual in-context reasoning in the bivariate case and demonstrates its potential.

**Limitations.** Our study is focused on controlled synthetic datasets to circumvent evaluation difficulties inherent to natural language. We only train on small-scale GPT-2 type model to demonstrate preliminary evidence on counterfactual story generation. Furthermore, we assume no observed confounders, which is difficult to satisfy in the real world, as observations are finite and contain missing information which requires *out-of-variable* generalization [Guo et al., 2023]. Realistic benchmarks on natural language evaluation and larger-scale pre-training that provide principled reasoning for real-world impact, such as scientific reasoning, represent potential avenues for future research.

**Broader impacts.** Since our models are not trained on natural language, the typical societal concerns associated with counterfactual story generation do not directly apply. We view our current work as a scientific exploration of desirable properties for the next generation of AI models.

## 7 Conclusion

We have discussed in-context counterfactual reasoning in both linear regression tasks and cyclic sequential data. We observed, regardless of RNN-like or Transformer-like architectures, that counterfactual reasoning can emerge in language models. We find that Transformers, in particular, rely on self-attention and model depth for in-context counterfactual reasoning. Data diversity in pre-training is essential for the emergence of reasoning and *OOD* generalization. We provide insights on how counterfactual reasoning can be interpreted as a copying and function estimation task, with theoretical and empirical evidence over a broad class of invertible functions (1). We introduce a sequential extension grounded in the Lotka–Volterra model of predator-prey dynamics [Lotka, 1910]. We show that both Transformers and RNNs can in-context learn such complex dynamics, and thus provide preliminary but concrete evidence on the potential for *counterfactual story generation* that is important to scientific discovery and AI safety.

## References

- J. Achiam, S. Adler, S. Agarwal, L. Ahmad, I. Akkaya, F. L. Aleman, D. Almeida, J. Altenschmidt, S. Altman, S. Anadkat, et al. Gpt-4 technical report. *arXiv preprint arXiv:2303.08774*, 2023. URL <https://arxiv.org/abs/2303.08774>.
- E. Akyürek, D. Schuurmans, J. Andreas, T. Ma, and D. Zhou. What learning algorithm is in-context learning? investigations with linear models. In *The Eleventh International Conference on Learning Representations*, 2023. URL <https://openreview.net/forum?id=0g0X4H8yN4I>.
- E. Akyürek, B. Wang, Y. Kim, and J. Andreas. In-context language learning: Architectures and algorithms. In *Forty-first International Conference on Machine Learning*, 2024. URL <https://openreview.net/forum?id=3Z9Crr5srL>.
- L. Bottou and B. Schölkopf. The fiction machine, April 2025. URL <https://www.siam.org/publications/siam-news/articles/the-fiction-machine/>.
- T. Brown, B. Mann, N. Ryder, M. Subbiah, J. D. Kaplan, P. Dhariwal, A. Neelakantan, P. Shyam, G. Sastry, A. Askell, S. Agarwal, A. Herbert-Voss, G. Krueger, T. Henighan, R. Child, A. Ramesh, D. Ziegler, J. Wu, C. Winter, C. Hesse, M. Chen, E. Sigler, M. Litwin, S. Gray, B. Chess, J. Clark, C. Berner, S. McCandlish, A. Radford, I. Sutskever, and D. Amodei. Language models are few-shot learners. In H. Larochelle, M. Ranzato, R. Hadsell, M. Balcan, and H. Lin, editors, *Advances in Neural Information Processing Systems*, volume 33, pages 1877–1901. Curran Associates, Inc., 2020. URL [https://proceedings.neurips.cc/paper\\_files/paper/2020/file/1457c0d6bfc4967418bfb8ac142f64a-Paper.pdf](https://proceedings.neurips.cc/paper_files/paper/2020/file/1457c0d6bfc4967418bfb8ac142f64a-Paper.pdf).
- L. Charleux, E. Roux, T. Goyallon, G. Feverati, and P. Nagorny. Lotka-volterra equations, 2018. URL [https://scientific-python.readthedocs.io/en/latest/notebooks\\_rst/3\\_Ordinary\\_Differential\\_Equations/02\\_Examples/Lotka\\_Volterra\\_model.html](https://scientific-python.readthedocs.io/en/latest/notebooks_rst/3_Ordinary_Differential_Equations/02_Examples/Lotka_Volterra_model.html).
- K. Cho, B. van Merriënboer, C. Gulcehre, D. Bahdanau, F. Bougares, H. Schwenk, and Y. Bengio. Learning phrase representations using RNN encoder–decoder for statistical machine translation. In A. Moschitti, B. Pang, and W. Daelemans, editors, *Proceedings of the 2014 Conference on Empirical Methods in Natural Language Processing (EMNLP)*, pages 1724–1734, Doha, Qatar, Oct. 2014. Association for Computational Linguistics. doi: 10.3115/v1/D14-1179. URL <https://aclanthology.org/D14-1179/>.
- D. Dai, Y. Sun, L. Dong, Y. Hao, S. Ma, Z. Sui, and F. Wei. Why can GPT learn in-context? language models implicitly perform gradient descent as meta-optimizers. In *ICLR 2023 Workshop on Mathematical and Empirical Understanding of Foundation Models*, 2023. URL <https://openreview.net/forum?id=fzbHRjAd8U>.
- B. de Finetti. Funzione caratteristica di un fenomeno aleatorio. *Atti della R. Accademia Nazionale dei Lincei, Serie 6. Memorie, Classe di Scienze Fisiche, Matematiche e Naturale*, 4:251–299, 1931. URL <http://www.brunodefinetti.it/Opere/funzioneCaratteristica.pdf>.
- G. Deutch, N. Magar, T. Natan, and G. Dar. In-context learning and gradient descent revisited. In K. Duh, H. Gomez, and S. Bethard, editors, *Proceedings of the 2024 Conference of the North American Chapter of the Association for Computational Linguistics: Human Language Technologies (Volume 1: Long Papers)*, pages 1017–1028, Mexico City, Mexico, June 2024. Association for Computational Linguistics. doi: 10.18653/v1/2024.naacl-long.58. URL <https://aclanthology.org/2024.naacl-long.58/>.
- B. Efron. Bootstrap methods: Another look at the jackknife. *The Annals of Statistics*, 7(1):1–26, 1979. ISSN 00905364, 21688966. URL <http://www.jstor.org/stable/2958830>.
- N. Elhage, N. Nanda, C. Olsson, T. Henighan, N. Joseph, B. Mann, A. Askell, Y. Bai, A. Chen, T. Conerly, N. DasSarma, D. Drain, D. Ganguli, Z. Hatfield-Dodds, D. Hernandez, A. Jones, J. Kernion, L. Lovitt, K. Ndousse, D. Amodei, T. Brown, J. Clark, J. Kaplan, S. McCandlish, and C. Olah. A mathematical framework for transformer circuits. *Transformer Circuits Thread*, 2021. URL <https://transformer-circuits.pub/2021/framework/index.html>.
- J. L. Elman. Finding structure in time. *Cognitive Science*, 14(2):179–211, 1990. URL [https://onlinelibrary.wiley.com/doi/abs/10.1207/s15516709cog1402\\_1](https://onlinelibrary.wiley.com/doi/abs/10.1207/s15516709cog1402_1).

- F. Falck, Z. Wang, and C. C. Holmes. Is in-context learning in large language models bayesian? A martingale perspective. In R. Salakhutdinov, Z. Kolter, K. Heller, A. Weller, N. Oliver, J. Scarlett, and F. Berkenkamp, editors, *Proceedings of the 41st International Conference on Machine Learning*, volume 235 of *Proceedings of Machine Learning Research*, pages 12784–12805. PMLR, 21–27 Jul 2024. URL <https://proceedings.mlr.press/v235/falck24a.html>.
- S. Garg, D. Tsipras, P. Liang, and G. Valiant. What can transformers learn in-context? a case study of simple function classes. In *Proceedings of the 36th International Conference on Neural Information Processing Systems, NIPS '22*, Red Hook, NY, USA, 2022. Curran Associates Inc. ISBN 9781713871088. URL <https://openreview.net/pdf?id=f1NZJ2e0et>.
- M. Grendar. Entropy and effective support size. *Entropy*, 8(3):169–174, 2006. ISSN 1099-4300. doi: 10.3390/e8030169. URL <https://www.mdpi.com/1099-4300/8/3/169>.
- S. Guo, J. B. Wildberger, and B. Schölkopf. Out-of-variable generalisation for discriminative models. In *The Twelfth International Conference on Learning Representations*, 2023. URL <https://openreview.net/pdf?id=zwMfg9PfPs>.
- S. Guo, V. Tóth, B. Schölkopf, and F. Huszár. Causal de finetti: On the identification of invariant causal structure in exchangeable data, 2024a. URL <https://arxiv.org/abs/2203.15756>.
- S. Guo, C. Zhang, K. Mohan, F. Huszár, and B. Schölkopf. Do finetti: On causal effects for exchangeable data, 2024b. URL <https://arxiv.org/abs/2405.18836>.
- M. A. Hernan. *Causal Inference: What If*. Taylor & Francis, Boca Raton, 2024. URL <https://miguelhernan.org/whatifbook>.
- S. Hochreiter and J. Schmidhuber. Long short-term memory. *Neural Computation*, 9(8):1735–1780, 1997. URL <https://www.bioinf.jku.at/publications/older/2604.pdf>.
- D. P. Kingma and J. Ba. Adam: A method for stochastic optimization. In Y. Bengio and Y. LeCun, editors, *3rd International Conference on Learning Representations, ICLR 2015, San Diego, CA, USA, May 7-9, 2015, Conference Track Proceedings*, 2015. URL <http://arxiv.org/abs/1412.6980>.
- A. Klenke. *Probability Theory: A Comprehensive Course*. Springer, 2008. URL <https://link.springer.com/book/10.1007/978-1-84800-048-3>.
- M. J. Kusner, J. Loftus, C. Russell, and R. Silva. Counterfactual fairness. *Advances in neural information processing systems*, 30, 2017. URL [https://proceedings.neurips.cc/paper\\_files/paper/2017/file/a486cd07e4ac3d270571622f4f316ec5-Paper.pdf](https://proceedings.neurips.cc/paper_files/paper/2017/file/a486cd07e4ac3d270571622f4f316ec5-Paper.pdf).
- J. Li, L. Yu, and A. Ettinger. Counterfactual reasoning: Testing language models’ understanding of hypothetical scenarios. In A. Rogers, J. Boyd-Graber, and N. Okazaki, editors, *Proceedings of the 61st Annual Meeting of the Association for Computational Linguistics (Volume 2: Short Papers)*, pages 804–815, Toronto, Canada, July 2023. Association for Computational Linguistics. doi: 10.18653/v1/2023.acl-short.70. URL <https://aclanthology.org/2023.acl-short.70/>.
- X. Li, T.-K. L. Wong, R. T. Q. Chen, and D. Duvenaud. Scalable gradients for stochastic differential equations. *International Conference on Artificial Intelligence and Statistics*, 2020. URL <https://proceedings.mlr.press/v108/li20i/li20i.pdf>.
- L. Lorch, A. Krause, and B. Schölkopf. Causal modeling with stationary diffusions. In S. Dasgupta, S. Mandt, and Y. Li, editors, *Proceedings of The 27th International Conference on Artificial Intelligence and Statistics*, volume 238 of *Proceedings of Machine Learning Research*, pages 1927–1935. PMLR, 02–04 May 2024. URL <https://proceedings.mlr.press/v238/lorch24a.html>.
- K. Lorenz. *Die Rückseite des Spiegels : Versuch einer Naturgeschichte menschlichen Erkennens*. Piper, München [u.a, 2. aufl. edition, 1973. ISBN 3492020305.
- A. J. Lotka. Contribution to the theory of periodic reactions. *The Journal of Physical Chemistry*, 14(3):271–274, 03 1910. doi: 10.1021/j150111a004. URL <https://doi.org/10.1021/j150111a004>.

- C. Lu, B. Huang, K. Wang, J. M. Hernández-Lobato, K. Zhang, and B. Schölkopf. Sample-efficient reinforcement learning via counterfactual-based data augmentation. In *Offline Reinforcement Learning - Workshop at the 34th Conference on Neural Information Processing Systems (NeurIPS)*, 2020. URL <https://offline-rl-neurips.github.io/pdf/34.pdf>.
- G. Maruyama. Continuous markov processes and stochastic equations. *Rendiconti del Circolo Matematico di Palermo*, 4(1):48–90, 1955. doi: 10.1007/BF02846028. URL <https://doi.org/10.1007/BF02846028>.
- T. Mesnard, T. Weber, F. Viola, S. Thakoor, A. Saade, A. Harutyunyan, W. Dabney, T. S. Stepleton, N. Heess, A. Guez, E. Moulines, M. Hutter, L. Buesing, and R. Munos. Counterfactual credit assignment in model-free reinforcement learning. In M. Meila and T. Zhang, editors, *Proceedings of the 38th International Conference on Machine Learning*, volume 139 of *Proceedings of Machine Learning Research*, pages 7654–7664. PMLR, 18–24 Jul 2021. URL <https://proceedings.mlr.press/v139/mesnard21a.html>.
- J. Mooij, D. Janzing, and B. Schölkopf. From ordinary differential equations to structural causal models: the deterministic case. In A. Nicholson and P. Smyth, editors, *Proceedings of the Twenty-Ninth Conference Annual Conference on Uncertainty in Artificial Intelligence*, pages 440–448, Corvallis, OR, 2013. AUAI Press. URL [http://www.is.tuebingen.mpg.de/fileadmin/user\\_upload/files/publications/2013/MooijJS2013-uai.pdf](http://www.is.tuebingen.mpg.de/fileadmin/user_upload/files/publications/2013/MooijJS2013-uai.pdf).
- C. Olsson, N. Elhage, N. Nanda, N. Joseph, N. DasSarma, T. Henighan, B. Mann, A. Askell, Y. Bai, A. Chen, T. Conerly, D. Drain, D. Ganguli, Z. Hatfield-Dodds, D. Hernandez, S. Johnston, A. Jones, J. Kernion, L. Lovitt, K. Ndousse, D. Amodei, T. Brown, J. Clark, J. Kaplan, S. McCandlish, and C. Olah. In-context learning and induction heads, 2022. URL <https://arxiv.org/abs/2209.11895>.
- A. Paszke, S. Gross, F. Massa, A. Lerer, J. Bradbury, G. Chanan, T. Killeen, Z. Lin, N. Gimelshein, L. Antiga, A. Desmaison, A. Köpf, E. Yang, Z. DeVito, M. Raison, A. Tejani, S. Chilamkurthy, B. Steiner, L. Fang, J. Bai, and S. Chintala. *PyTorch: an imperative style, high-performance deep learning library*. Curran Associates Inc., Red Hook, NY, USA, 2019. URL [https://proceedings.neurips.cc/paper\\_files/paper/2019/file/bdbca288fee7f92f2bfa9f7012727740-Paper.pdf](https://proceedings.neurips.cc/paper_files/paper/2019/file/bdbca288fee7f92f2bfa9f7012727740-Paper.pdf).
- J. Pearl. *Causality: Models, Reasoning and Inference*. Cambridge University Press, 2nd edition, 2009. URL <https://bayes.cs.ucla.edu/B00K-2K/>.
- J. Peters, D. Janzing, and B. Schölkopf. Causal inference on discrete data using additive noise models. *IEEE Transactions on Pattern Analysis and Machine Intelligence*, 33(12):2436–2450, 2011. URL <https://ieeexplore.ieee.org/document/5740928>.
- J. Peters, J. M. Mooij, D. Janzing, and B. Schölkopf. Causal discovery with continuous additive noise models. *The Journal of Machine Learning Research*, 15(1):2009–2053, 2014. URL <https://jmlr.org/papers/volume15/peters14a/peters14a.pdf>.
- J. Peters, S. Bauer, and N. Pfister. *Causal Models for Dynamical Systems*, page 671–690. Association for Computing Machinery, New York, NY, USA, 1 edition, 2022. ISBN 9781450395861. URL <https://doi.org/10.1145/3501714.3501752>.
- L. Qin, A. Bosselut, A. Holtzman, C. Bhagavatula, E. Clark, and Y. Choi. Counterfactual story reasoning and generation. In K. Inui, J. Jiang, V. Ng, and X. Wan, editors, *Proceedings of the 2019 Conference on Empirical Methods in Natural Language Processing and the 9th International Joint Conference on Natural Language Processing (EMNLP-IJCNLP)*, pages 5043–5053, Hong Kong, China, Nov. 2019. Association for Computational Linguistics. doi: 10.18653/v1/D19-1509. URL <https://aclanthology.org/D19-1509/>.
- A. Radford, J. Wu, R. Child, D. Luan, D. Amodei, and I. Sutskever. Language models are unsupervised multitask learners. 2019. URL [https://cdn.openai.com/better-language-models/language\\_models\\_are\\_unsupervised\\_multitask\\_learners.pdf](https://cdn.openai.com/better-language-models/language_models_are_unsupervised_multitask_learners.pdf). OpenAI Technical Report.

- S. Ravfogel, A. Svete, V. Snæbjarnarson, and R. Cotterell. Gumbel counterfactual generation from language models. In *The Thirteenth International Conference on Learning Representations*, 2025. URL <https://openreview.net/forum?id=TUC0ZT2zIQ>.
- P. Reizinger, S. Guo, F. Huszár, B. Schölkopf, and W. Brendel. Identifiable exchangeable mechanisms for causal structure and representation learning. In *The Thirteenth International Conference on Learning Representations*, 2025. URL <https://openreview.net/forum?id=k03mB41vyM>.
- A. Sauer and A. Geiger. Counterfactual generative networks. In *International Conference on Learning Representations*, 2021. URL <https://openreview.net/forum?id=BXewfAYMmJw>.
- B. Schölkopf. Causality for machine learning. In *Probabilistic and causal inference: The works of Judea Pearl*, pages 765–804. 2022. URL <https://dl.acm.org/doi/10.1145/3501714.3501755>.
- C. E. Shannon. A mathematical theory of communication. *The Bell System Technical Journal*, 27(3):379–423, 1948. URL <https://people.math.harvard.edu/~ctm/home/text/others/shannon/entropy/entropy.pdf>.
- V. Southgate and A. Verneti. Belief-based action prediction in preverbal infants. *Cognition*, 130(1):1–10, 2014. URL <https://www.sciencedirect.com/science/article/pii/S0010027713001650?via%3Dihub>.
- N. Tandon, B. Dalvi, K. Sakaguchi, P. Clark, and A. Bosselut. WIQA: A dataset for “what if...” reasoning over procedural text. In K. Inui, J. Jiang, V. Ng, and X. Wan, editors, *Proceedings of the 2019 Conference on Empirical Methods in Natural Language Processing and the 9th International Joint Conference on Natural Language Processing (EMNLP-IJCNLP)*, pages 6076–6085, Hong Kong, China, Nov. 2019. Association for Computational Linguistics. doi: 10.18653/v1/D19-1629. URL <https://aclanthology.org/D19-1629/>.
- A. Vaswani, N. Shazeer, N. Parmar, J. Uszkoreit, L. Jones, A. N. Gomez, L. Kaiser, and I. Polosukhin. Attention is all you need. In *Proceedings of the 31st International Conference on Neural Information Processing Systems, NIPS’17*, page 6000–6010, Red Hook, NY, USA, 2017. Curran Associates Inc. ISBN 9781510860964. URL [https://proceedings.neurips.cc/paper\\_files/paper/2017/file/3f5ee243547dee91fbd053c1c4a845aa-Paper.pdf](https://proceedings.neurips.cc/paper_files/paper/2017/file/3f5ee243547dee91fbd053c1c4a845aa-Paper.pdf).
- J. von Oswald, E. Niklasson, E. Randazzo, J. a. Sacramento, A. Mordvintsev, A. Zhmoginov, and M. Vladymyrov. Transformers learn in-context by gradient descent. In *Proceedings of the 40th International Conference on Machine Learning, ICML’23*. JMLR.org, 2023. URL <https://proceedings.mlr.press/v202/von-oswald23a/von-oswald23a.pdf>.
- S. Wachter, B. Mittelstadt, and C. Russell. Counterfactual explanations without opening the black box: Automated decisions and the gdpr. *Harv. JL & Tech.*, 31:841, 2017. URL <https://arxiv.org/pdf/1711.00399>.
- S. M. Xie, A. Raghunathan, P. Liang, and T. Ma. An explanation of in-context learning as implicit bayesian inference, 2022. URL <https://arxiv.org/abs/2111.02080>.
- H. Yan, L. Kong, L. Gui, Y. Chi, E. Xing, Y. He, and K. Zhang. Counterfactual generation with identifiability guarantees. In *Thirty-seventh Conference on Neural Information Processing Systems*, 2023. URL <https://openreview.net/forum?id=cslnCXE9XA>.
- N. Ye and H. Namkoong. Exchangeable sequence models quantify uncertainty over latent concepts, 2024. URL <https://arxiv.org/abs/2408.03307>.
- L. Zhang, R. T. McCoy, T. R. Sumers, J.-Q. Zhu, and T. L. Griffiths. Deep de finetti: Recovering topic distributions from large language models, 2023. URL <https://arxiv.org/abs/2312.14226>.

## A Posterior predictive distribution

*Proof of posterior predictive distribution.* Let  $\Theta \subset \mathbb{R}$ ,  $B \subseteq \mathbb{R}$  and  $\beta \in B$ . Define the observational data  $\mathbf{x} = (x_1, y_1, \dots, x_n, y_n)$ . Then, with query  $:= (x_1, y_1, \dots, x_n, y_n, z, x^{\text{CF}})$ ,

$$\begin{aligned} p_{Y_Z^{\text{CF}}}(y_z^{\text{CF}}|\text{query}) &= \int_{\Theta} p_{Y_Z^{\text{CF}}}(y_z^{\text{CF}}|\text{query}, \theta) \pi(\theta|\text{query}) d\theta \\ &= \int_{\Theta} p_{Y_Z^{\text{CF}}}(y_z^{\text{CF}}|\mathbf{x}, \theta, x_z^{\text{CF}}, z) \pi(\theta|\mathbf{x}, x_z^{\text{CF}}, z) d\theta \\ &\stackrel{\text{II}}{=} \int_{\Theta} p_{Y_Z^{\text{CF}}}(y_z^{\text{CF}}|\mathbf{x}, \theta, x_z^{\text{CF}}, z) \pi(\theta|\mathbf{x}) d\theta \end{aligned} \quad (7)$$

$$\begin{aligned} &= \int_{\Theta} \int_B p_{Y_Z^{\text{CF}}}(\beta(x_z^{\text{CF}} - x_z) + y_z|\mathbf{x}, \theta, x_z^{\text{CF}}, z, \beta) p_{\beta}(\beta|\mathbf{x}, \theta, x_z^{\text{CF}}, z) \pi(\theta|\mathbf{x}) d\beta d\theta \\ &\stackrel{\text{dF}}{=} \int_{\Theta} \int_B p_{Y_Z^{\text{CF}}}(\beta(x_z^{\text{CF}} - x_z) + y_z|x_i, y_i, \theta, x_z^{\text{CF}}, z, \beta) p_{\beta}(\beta|\mathbf{x}, \theta) \pi(\theta|\mathbf{x}) d\beta d\theta \quad (8) \\ &= \int_{\Theta} \int_B \delta(Y_Z^{\text{CF}} = \beta x_z^{\text{CF}} + y_z - \beta x_z) p_{\beta}(\beta|\mathbf{x}, \theta) \pi(\theta|\mathbf{x}) d\beta d\theta, \end{aligned}$$

where (7) follows by independence, as  $\theta \perp\!\!\!\perp (X^{\text{CF}}, Z)$ , and (8) by de Finetti [de Finetti, 1931, Klenke, 2008], as the in-context examples  $((x_1, y_1), \dots, (x_n, y_n))$  are exchangeable.  $\square$

*Mean and variance in linear additive framework.* Both follow immediately by the tower law (III) of iterated expectations,

$$\begin{aligned} \mathbb{E}[Y^{\text{CF}}] &= \mathbb{E}[\beta X^{\text{CF}} + U_Y] \\ &\stackrel{\text{III}}{=} \mathbb{E}[\mathbb{E}[\beta|\theta]] \mathbb{E}[X^{\text{CF}}] + \mathbb{E}[\mathbb{E}[U_Y|\theta]] \\ &= \mathbb{E}[\theta] = 0 \\ \text{Var}(Y^{\text{CF}}) &= \mathbb{E}[(Y^{\text{CF}})^2] = \mathbb{E}[(\beta X^{\text{CF}} + U_Y)^2] \\ &= \mathbb{E}[(\beta X^{\text{CF}})^2 + 2\beta X^{\text{CF}} U_Y + U_Y^2] \\ &\stackrel{\text{II}}{=} \mathbb{E}[\beta^2] \mathbb{E}[(X^{\text{CF}})^2] + 2\mathbb{E}[\beta U_Y] \mathbb{E}[X^{\text{CF}}] + \mathbb{E}[U_Y^2] \\ &\stackrel{\text{III}}{=} \mathbb{E}[\mathbb{E}[\beta^2|\theta]] \text{Var}(X^{\text{CF}}) + \mathbb{E}[\mathbb{E}[U_Y^2|\theta]] \\ &= \mathbb{E}[1 + \theta^2] (\text{Var}(X^{\text{CF}}) + 1) \\ &= (1 + \text{Var}(\theta))(12 + 1) = 13^2 = 169. \end{aligned}$$

The proof for the variance under the multiplicative extension,  $\text{Var}(\beta X^{\text{CF}} U_Y)$ , is analogous.  $\square$

## B Transformation lemma

*Proof of Lemma 1.* As  $T$  is invertible in  $U$  given  $f(X)$ ,

$$Y^{\text{CF}} = T(f(X^{\text{CF}}), U) = T(f(X^{\text{CF}}), T^{-1}(f(X), Y)).$$

We require injectivity in  $u$  to uniquely determine  $u$  from  $(f(X), Y)$ . Else,  $Y^{\text{CF}} = T(f(X^{\text{CF}}), u)$  is ambiguous and counterfactuals are ill-defined. Thus, the counterfactual completion writes

$$Y^{\text{CF}} = h(f(X), f(X^{\text{CF}}), Y)$$

for  $h : \mathcal{F} \times \mathcal{F} \times \mathcal{U} \longrightarrow \mathcal{Y}$ .  $\square$

## C Training details

We construct synthetic datasets with fixed noise. Conditional on a uniformly distributed latent parameter  $\theta_i \in \Theta$ , we draw  $n_i \sim \mathcal{U}(\{1, \dots, 50\})$  observational data points with noise  $\mathbf{U}_X^{i;j} | \theta_i, \mathbf{U}_Y^{i;j} | \theta_i \in \mathbb{R}^E, j \in \{1, \dots, n_i\}$  and weights  $\beta_i | \theta_i \in \mathbb{R}^E, i \in \{1, \dots, N \cdot B\}$  to enforce *non-i.i.d.* data. We choose  $E = 5$ . Next, we sample  $N \cdot B$  data points with

$$\begin{aligned} \theta &\sim \mathcal{U}([-6, 6]^E) & \beta | \theta &\sim \mathcal{N}(\theta, \mathbf{I}_E) \\ \mathbf{U} | \theta &\sim \mathcal{N}(\theta, \mathbf{I}_E) & \mathbf{X}^{\text{CF}} &\sim \mathcal{U}([-6, 6]^E) \end{aligned} \quad (9)$$

for  $N = 200000$  training steps of batch size  $B = 64$ . We set

$$\mathbf{Y} = \beta \odot \mathbf{U}_X + \mathbf{U}_Y$$

with  $\odot$  denoting element-wise products to have input and output embedding dimension agree without zero-padding. Including the indicator token  $Z_b = z_b \cdot \mathbf{1}_E, z_b \in \{1, \dots, n_b\}$ , the corpus of queries then consists of  $N$  batches of the form

$$\{(\mathbf{x}_{b;1}, \mathbf{y}_{b;1}, \dots, \mathbf{x}_{b;n_b}, \mathbf{y}_{b;n_b}, \mathbf{z}_b, \mathbf{x}_b^{\text{CF}})\}_{b \in \{1, \dots, B\}}$$

on which the model has to predict  $\mathbf{y}_{b;z_b}^{\text{CF}}, b \in \{1, \dots, B\} =: [B]$ . Our target  $Y^{\text{CF}}$  is zero-mean with  $\text{Var}(Y^{\text{CF}}) = 169$  and  $\log(\text{Var}(Y^{\text{CF}})) = 5.1299$ .

We train on minimizing the per-batch mean squared error (MSE) between the counterfactual prediction  $\widehat{\mathbf{y}}_{[B]}^{\text{CF}}$  and the ground truth  $\mathbf{y}_{[B]}^{\text{CF}}$ ,

$$\text{MSE}(\widehat{\mathbf{y}}_{[B]}^{\text{CF}}, \mathbf{y}_{[B]}^{\text{CF}}) = \frac{1}{B \cdot E} \sum_{b=1}^B \left\| \widehat{\mathbf{y}}_{b;z_b}^{\text{CF}} - \mathbf{y}_{b;z_b}^{\text{CF}} \right\|_2^2$$

and evaluate on an unseen test set following (9). We use the notational forms  $\text{MSE}(\widehat{y}, y)$  and  $\text{MSE}(\widehat{y} - y)$  interchangeably.

Our code is based on the repository by Garg et al. [2022]. We therefore adopt the Adam optimizer [Kingma and Ba, 2015] and a learning rate of  $10^{-4}$  for all function classes and models. We implement the experiments in pytorch [Paszke et al., 2019] and use one NVIDIA GeForce RTX 3090 GPU for training. All conducted experiments require between 10 minutes and 3 hours of training depending on model setup and task complexity.

### C.1 A note on embedding dimension $E$

Following the approach of Garg et al. [2022], we train models using various embedding dimensions and analyze their performance. For  $E = 20$ , we observe in-context performance that is comparable to the case with  $E = 5$ . However, training convergence is noticeably slower. In particular, for  $E = 50$ , the training loss has *not yet* fully converged after  $N = 200000$  steps. Similar trends are observed for  $E = 75$  and  $E = 100$ . For the model trained with  $E = 250$ , the training loss plateaus at a level consistent with the theoretical variance.

Given the extensive number of experiments conducted, we opt for a small embedding dimension of  $E = 5$ . This choice is especially important for experiments involving data diversity and cyclic causal structures, which are trained with fewer steps. In these cases, larger embedding dimensions would entail higher computational costs. Since our study relies on synthetic data, we prioritize efficiency and reproducibility by choosing a smaller  $E$ .

## D Model details

The Transformer architecture is described in subsection 2.2. Here we lay out the details on the three recurrent models used and investigate the relevance of model depth in Transformers more closely.

## D.1 Model details on RNN architectures

The Elman RNN [Elman, 1990] is a foundational recurrent neural network architecture. It consists of an input layer, a hidden layer with recurrent connections, and an output layer. The hidden state at time step  $t$ , denoted by  $h_t$ , is computed as

$$\begin{aligned} h_t &= \tanh(W_{ih}x_t + W_{hh}h_{t-1} + b_h) \\ y_t &= W_{ho}h_t + b_o, \end{aligned}$$

where  $x_t$  is the input at time  $t$ , and  $\tanh$  denotes the *tangens hyperbolicus*, a non-linear activation function. The output is given by  $y_t$  and  $W$ ,  $b$  represent learnable weight matrices and biases.

The Long Short-Term Memory (LSTM) network [Hochreiter and Schmidhuber, 1997] addresses the vanishing gradient problem by incorporating a memory cell and three gates: input ( $i_t$ ), forget ( $f_t$ ), and output ( $o_t$ ). These gates regulate the flow of information and enable the network to retain long-term dependencies. The LSTM cell is defined by the following equations,

$$\begin{aligned} f_t &= \sigma(W_fx_t + U_fh_{t-1} + b_f) \\ i_t &= \sigma(W_ix_t + U_ih_{t-1} + b_i) \\ o_t &= \sigma(W_ox_t + U_oh_{t-1} + b_o) \\ g_t &= \tanh(W_gx_t + U_gh_{t-1} + b_g) \\ c_t &= f_t \odot c_{t-1} + i_t \odot g_t \\ h_t &= o_t \odot \tanh(c_t). \end{aligned}$$

In this formulation,  $c_t$  is the cell state and  $h_t$  the hidden output state. Activation vectors of the three gates are given by  $i_t, f_t, o_t$  and  $g_t$  is the cell input activation vector. By  $\sigma$ , we denote the sigmoid function and element-wise multiplication by  $\odot$ .  $U$  represents another weight matrix.

The Gated Recurrent Unit (GRU) [Cho et al., 2014] introduces gating mechanisms to better control the flow of information. It simplifies the LSTM architecture by combining the forget and input gates into a single update gate,  $z_t$ . The GRU computes its hidden state using the following equations,

$$\begin{aligned} r_t &= \sigma(W_rx_t + U_rh_{t-1} + b_r) \\ z_t &= \sigma(W_zx_t + U_zh_{t-1} + b_z) \\ n_t &= \tanh(W_nx_t + U_n(r_t \odot h_{t-1}) + b_n) \\ h_t &= (1 - z_t) \odot n_t + z_t \odot h_{t-1}. \end{aligned}$$

Here,  $r_t$  is the reset gate,  $z_t$  the update gate,  $n_t$  the new gate, the candidate update vector. Note that the dependence of the hidden state on the update gate varies across documentations. We follow the definition in the `pytorch` package.

We perform a hyperparameter sweep on hidden size  $D$  and the number of layers  $L$  over the grid  $D \in \{64, 128, 256\}, L \in \{2, 3\}$ . We select the configuration with hidden size 256 and 3 layers for each of the three architectures. Figure 6 sheds more light on the performance results illustrated by Figure 2. For long contexts of at least 17 in-context examples, the Elman RNN achieves significantly higher in-context MSE than the three other architectures. For the LSTM, GRU and STANDARD Transformer, we observe no significant performance difference across models.

## D.2 Varying depth for additional values

Analogous to Figure 3b, we note that increasing model depth leads to declining in-context MSE. This holds for contexts both shorter and longer than the 35-example version considered above. Figure 7 illustrates the in-context MSE for varying depth, evaluated at 1 and 50 in-context examples, respectively. We note that the loss of the 1-layer, 8-head Transformer exhibits no significant differences between 1 in-context example and 50. We interpret this as indication that the model is unable to infer information on the latent  $\theta$  from the context. Reinforcing our findings that the 4-layer, 2-head and 8-layer, 1-head Transformers achieve the lowest in-context MSE, this pattern serves as evidence that in-context inference occurs across layers. A contrasting notion may be that the Transformer maps different junks of information to different subspaces of the embedding space. Acting on each subspace individually, each attention head would then focus on a different task before the MLP would combine the information and output the final prediction. Instead, the model appears to benefit from



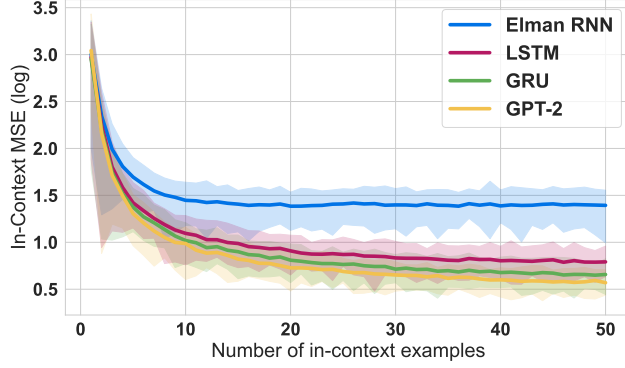
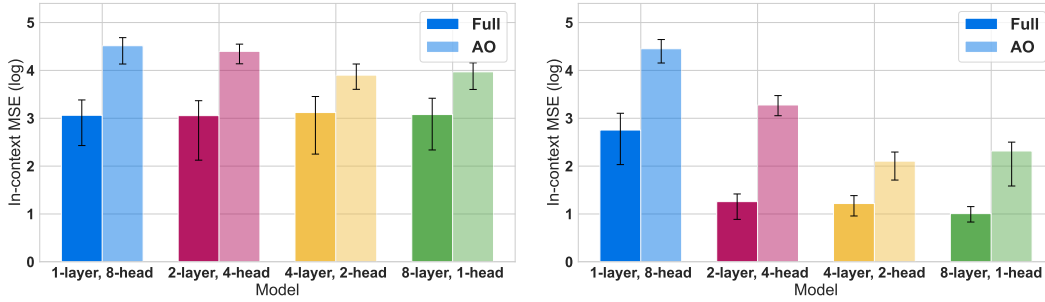


Figure 6: **Model comparisons for in-context counterfactual reasoning.** In-context counterfactual prediction accuracy measured via log-transformed mean-squared error loss averaged over 100 sequences versus the number of in-context examples observed in a prompt. We compare the following model architectures: GPT-2 (STANDARD), LSTM, GRU, and Elman RNN. All models are capable of in-context counterfactual reasoning. GPT-2 (STANDARD) achieves lowest error and fastest convergence rate for a small number of in-context examples. For more than 17 in-context examples, the Elman RNN has significantly [Efron, 1979] higher in-context MSE than the three other architectures.



(a) Varying depth for 1 in-context example.

(b) Varying depth for 50 in-context examples.

Figure 7: **Varying depth more closely.** Building on top of the results displayed in Figure 3b, we compare **Full** and **AO** Transformers at a constant number of 8 attention heads. We observe a decrease in in-context loss as model depth increases across shorter and longer contexts of 1 and 50 in-context examples, respectively. We evaluate on 100 sequences.

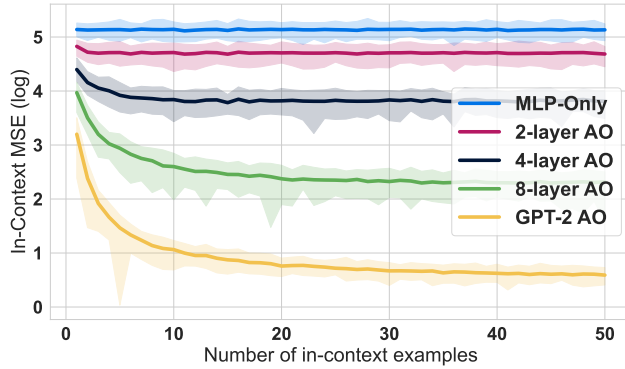


Figure 8: **Switching attention.** In-context MSE stagnates with increasing number of in-context examples observed for **MLP-Only** model. We compare to **AO** Transformers of 2, 4, 8 layers and the STANDARD GPT-2 setup. For all Transformers, in-context MSE decreases as more in-context examples are observed. Error bars are basic bootstrap confidence intervals [Efron, 1979].

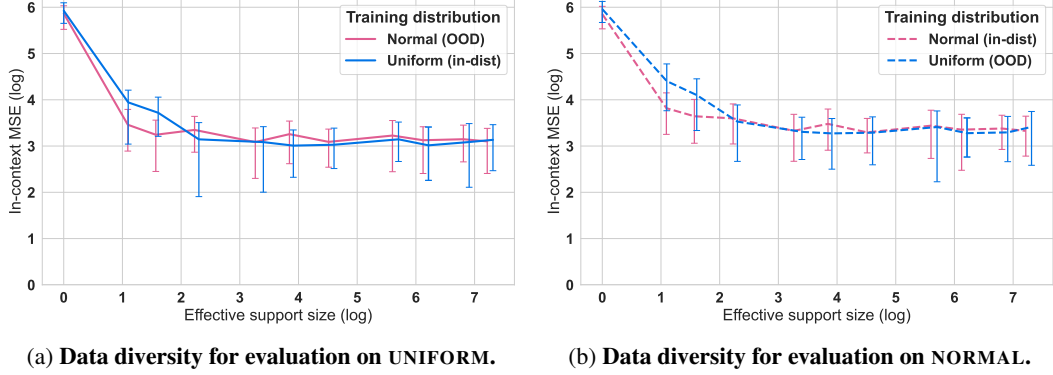


Figure 9: **Data diversity for pre-training on 1 in-context example.** We measure in-context MSE (log-scaled) averaged over 100 prompts at one in-context example against log-scaled effective support size. Each point represents one fully pre-trained model on either the UNIFORM sampled or NORMAL sampled  $\theta$ . We train the models for 50000 training steps. All models in are evaluated on both datasets. Error bars are the 95% basic bootstrap confidence intervals.

the interplay between layers, which supports the claim that attention heads across layers communicate through the residual stream [Elhage et al., 2021].

Figure 8 underscores the results illustrated by Figure 3a by indicating significant differences between the **MLP-Only** setting and each of the four considered **AO** Transformer variants.

## E Data diversity and robustness

### E.1 Data diversity adjustments and out-of-distribution

In 4.3, we discuss data diversity and generalizability to *OOD*. The UNIFORM setup largely follows the overall setup described in (9) with the following adjustment: instead of  $N \cdot B \cdot E$ , we sample  $d \ll N$  realizations of the latent and compute the effective support size [Grendar, 2006]. Note that we control the absolute number of one-dimensional realizations as our setup effectively analyzes  $E$  independent examples at every turn. Thus, we draw  $d$  realizations and allocate across iterations and embedding dimensions. The parameter  $d$  corresponds to the diversity argument in our code.

The NORMAL setup follows the above structure. Compared to (9), we sample the latent from  $\theta \sim \mathcal{N}(\mathbf{0}, \sqrt{12} \cdot \mathbf{I}_E)$  such that the theoretical variance is equivalent across setups. Everything else is analogous. Note that the effective support size is equivalent to the support size under the UNIFORM setup. This can be seen by interpreting Ess as the logarithm of the Shannon entropy. Indeed,  $p(\vartheta)$  is uniformly distributed over discrete  $\Theta_0$  if  $\vartheta$  denotes a realization of the latent  $\theta$ ,

$$H_{\text{UNIFORM}}(\theta) = - \sum_{\vartheta \in \Theta_0} \log p(\vartheta).$$

Therefore, we allocate the  $d = |\Theta_0|$  realizations uniformly across iterations and embedding dimensions. Under the NORMAL setup,  $p(\vartheta)$  depends on the distance of  $\vartheta$  to 0. Here, we sample  $d$  Gaussian realizations. We then allocate them proportional to  $p(\vartheta)$  across iterations and embedding dimensions. In analogy to Figure 4, we plot the in-context MSE against Ess for pre-training on the NORMAL setting and evaluating both in-distribution and on UNIFORM. Figure 9 illustrates the in-context MSE relative to effective support size on contexts of one example. Here we train all models for 50000 training steps. Although the loss is at a higher level than for 35 in-context examples, we observe that the MSE declines with increasing effective support size. In terms of sufficient data diversity, the findings are consistent with above, as we require pre-training effective support size of around 10.

### E.2 Non-linear and non-additive extensions

On top of the linear regression setting, we extend in-context counterfactual reasoning to non-linear, non-additive functions which are invertible in  $u$ . The general dataset setup remains the same with

adjustments made only to the computation of  $y, y^{\text{CF}}$ . We evaluate the the 8-layer, 1-head **Full** and **AO** Transformers. Table 1 reports the in-context MSE on 100 queries with 35 in-context examples each. Depending on the exact configuration of architecture and extension, the in-context MSE is at least one tenth of the empirical variance of the test set.

	$f(x, u)$	Empirical variance	MSE of <b>AO</b> Transformer	MSE of <b>Full</b> Transformer
Tanh	$\tanh(\tau(\beta x + u))$	0.3144	0.0186	0.0058
Sigmoid ( $\sigma$ )	$\frac{1}{1 + \exp(-\tau(\beta x + u))}$	0.0355	0.0016	0.0005
Multiplicative	$\frac{1}{\sqrt{\text{Var}(\beta X^{\text{CF}} U_Y)}} \beta x u$	0.7888	0.0671	0.0437

Table 1: **Robustness to different function classes for regression tasks.** We report in-context MSE averaged over 100 sequences for the 8-layer **AO** and **Full** Transformers under invertible nonlinear activation functions and multiplicative noise. We compute the empirical variance of target  $Y^{\text{CF}}$  on the test set. We observe for both architectures that the MSE is 10 to 70 times lower than the empirical variance, suggesting both can in-context learn more complex function classes beyond linear regression and complete the counterfactual query. All functions are applied element-wise in one dimension.  $\tanh$  and  $\sigma$  are scaled by  $\tau = \frac{1}{13}$  to counteract congestion around  $\{-1, 1\}$  and  $\{0, 1\}$ , respectively. To guarantee theoretical variance of 1, we divide the multiplicative term by  $\sqrt{\text{Var}(\beta X^{\text{CF}} U_Y)} = \sqrt{3410.4}$ .

Note that under multiplicative noise, counterfactual reasoning reduces to a pure copying task as

$$Y^{\text{CF}} = \frac{1}{\sqrt{\text{Var}(Y^{\text{CF}})}} \beta X^{\text{CF}} U_Y = \frac{1}{\sqrt{\text{Var}(Y^{\text{CF}})}} \beta X^{\text{CF}} \frac{Y \sqrt{\text{Var}(Y^{\text{CF}})}}{\beta X} = \frac{X^{\text{CF}}}{X} Y,$$

where estimation of  $\beta$  is not required for counterfactual completion.

## F Model details for cyclic sequential dynamical systems

### F.1 Training details

In accordance with our exchangeable setting, we construct the dataset

$$\begin{aligned} \theta &\sim \mathcal{U}([1, 2]^E) & \alpha, \beta, \gamma, \delta | \theta &\sim \text{Exp}(\theta) \\ \mathbf{U} | \theta &\sim \mathcal{N}(\theta, \mathbf{I}_E) & \mathbf{X}^{\text{CF}} &\sim \mathcal{U}([1, 2]^E) \end{aligned} \quad (10)$$

where we sample  $N_i \sim \text{Pois}(\lambda)$  distinct time steps for  $i \in \{1, \dots, N \cdot B\}$  and  $\lambda = 200$ . We truncate the sequence on  $[0, 0.1]$  to overcome exploding concentrations and obtain the expected number of distinct time steps  $\mathbb{E}[N_i] = 0.1 \cdot 200 = 20$ . We again consider  $E$  independent sequences at once by stacking independent one-dimensional SDEs. Within one example, all SDEs are evaluated at the same distinct time steps. At any  $i$ , we then provide the observational sequence as

$$(\mathbf{x}_0, \mathbf{y}_0, \mathbf{x}_{t_1}, \mathbf{y}_{t_1}, \dots, \mathbf{x}_{t_{N_i}}, \mathbf{y}_{t_{N_i}}, \mathbf{z}, \mathbf{x}_0^{\text{CF}}, \mathbf{y}_0^{\text{CF}})$$

for  $\mathbf{z}$  a counterfactual delimiter token, identical across  $i$ . Given the query, we ask the model to predict the *full* completion of the counterfactual sequence,  $\text{comp}_i := (\mathbf{x}_{t_1}^{\text{CF}}, \mathbf{y}_{t_1}^{\text{CF}}, \dots, \mathbf{x}_{t_{N_i}}^{\text{CF}}, \mathbf{y}_{t_{N_i}}^{\text{CF}})$ , autoregressively. We again evaluate the model on the per-batch MSE of the predicted completion,  $\widehat{\text{comp}}_{[B]}$ , and the underlying ground truth sequence,  $\text{comp}_{[B]}$ ,

$$\text{MSE}(\widehat{\text{comp}}_{[B]}, \text{comp}_{[B]}) = \frac{1}{B \cdot E} \sum_{b=1}^B \|\widehat{\text{comp}}_b - \text{comp}_b\|_2^2$$

and evaluate on an unseen test set following (10).

We train for  $N = 10000$  training steps at batch size of  $B = 64$  and numerically approximate the solutions to the SDEs in (3) using the Euler–Maruyama [Maruyama, 1955] scheme. The counterfactual sequence is generated analogously but by recycling the Brownian motion used for the observational sequence. The manifestation of this can be seen in Figure 5b as *observational* and *counterfactual*  $y$  exhibit corresponding dynamics at each realized time step  $t_n \leq t_{N_i}$ . We inherit the `torchsde` package from Li et al. [2020] and follow Charleux et al. [2018] for the implementation of the Lotka-Volterra equations. All other specifications are similar to the regression setup described in Appendix C.

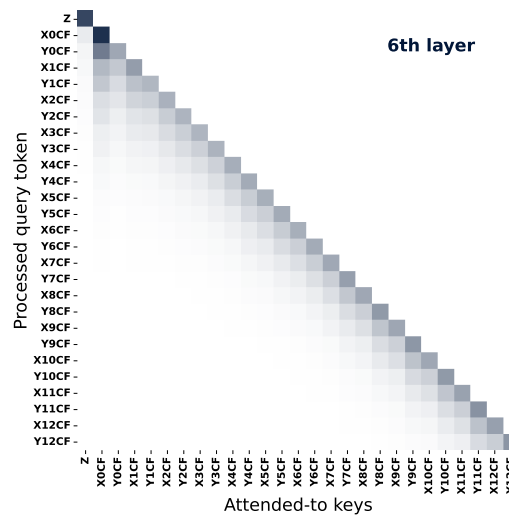
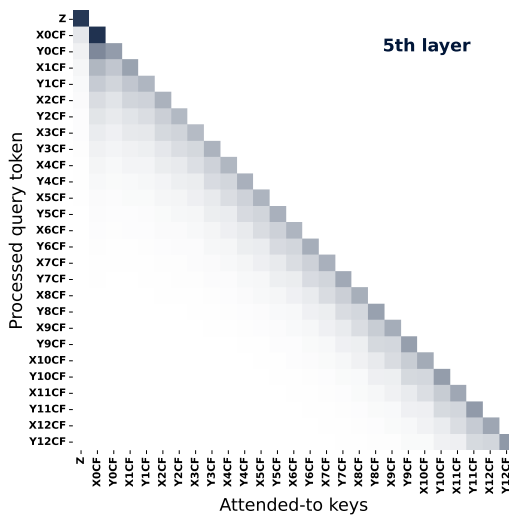
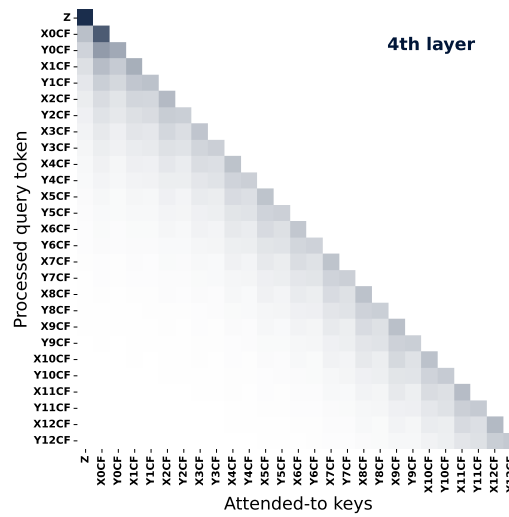
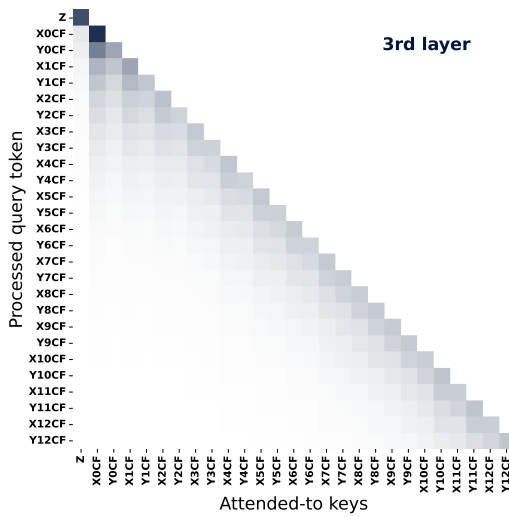
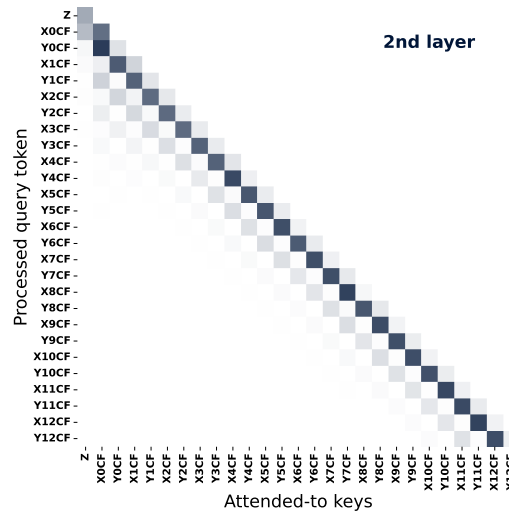
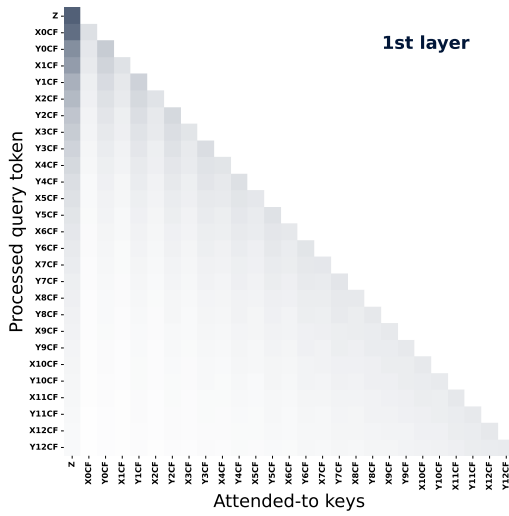
## F.2 Lotka-Volterra model

The Lotka-Volterra framework models the temporal evolution of the concentrations of two interacting species: predators and prey. In the absence of predators, the prey concentration grows continuously over time. Conversely, the predator concentration declines unless sustained by consuming prey. Predation enables predator growth, which simultaneously reduces prey concentration. We model the four individual dynamics by real, nonnegative parameters. The dynamics of the prey concentration (5) is parameterized by the intrinsic growth rate  $\alpha$  and the rate at which the prey concentration decreases with predator concentration,  $\beta$ . For predator concentration (6), we capture the species-inherent decreasing concentration by  $\gamma$  and the rate at which predators feed off prey by  $\delta$ . In the context of biological species, *concentration* can be thought of as the population density.

## F.3 Attention behavior

Figure 11 shows that the 8-layer, 1-head **AO** Transformer performs counterfactual reasoning by repeatedly moving information forward. Trained on variable sequence length, the model exhibits this pattern for different context lengths. Across a diverse set of test sequences, we observe that the tokens of the counterfactual sequence attend to the position of the delimiter token **z** at the first layer. Note that we only plot attention values between tokens of the counterfactual sequence. The Transformer at the second layer implements an induction head [Olsson et al., 2022] that copies forward the information one step. Then, we find five attention heads which implement decaying attention over prior positions. Maximum weight is here put on the current token, and progressively lower weights on all previous tokens relative to token distance. This design facilitates forward information propagation across tokens. The final attention head aggregates signals from the current and preceding token, integrating both token-specific information and temporally local context shared within the token pair at time  $t_n$ .

In accordance with the hypothesis that induction heads drive in-context learning [Elhage et al., 2021, Olsson et al., 2022, Akyürek et al., 2024], we notice this pattern for larger models, with multiple heads per layer, and including the MLP. For instance, the **Full** STANDARD GPT-2 Transformer contains three heads across the first two layers which mostly attend to the delimiter token **z**. At the third layer, the model implements an induction head. Taken together, this provides more evidence that counterfactual reasoning emerges, at least partly, in the self-attention layer of the Transformer.



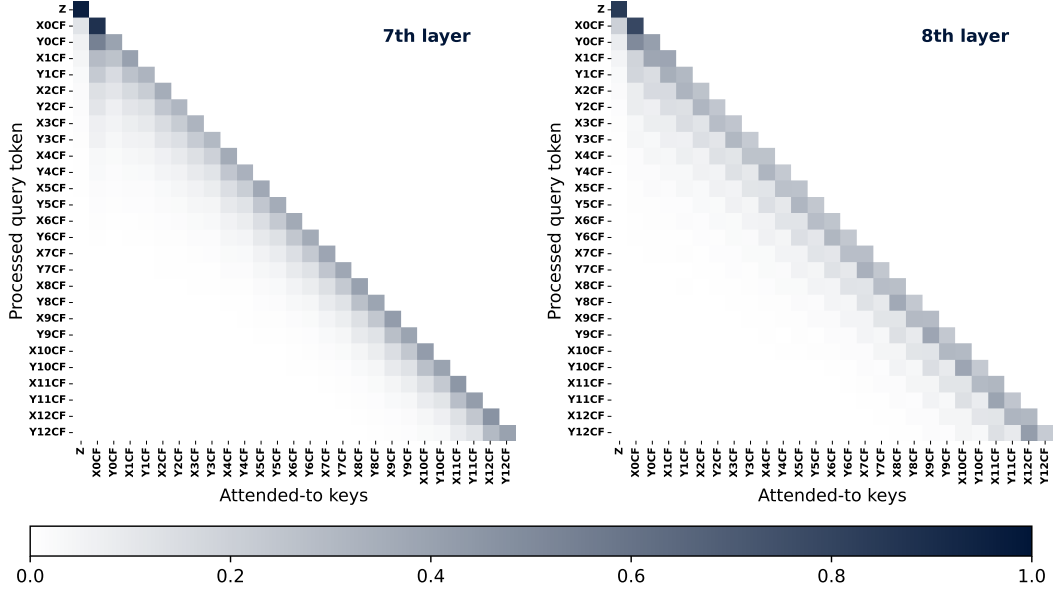


Figure 11: **Cyclic causal relationship.** The 8-layer AO Transformer, trained on counterfactual reasoning in Lotka-Volterra SDEs, includes two dedicated copying heads. At layer 2, the induction head shifts residual stream information from the previous token forward one position. The subsequent five attention heads implement decaying attention over prior positions, with maximum weight on the current token and progressively lower weights on all previous tokens relative to token distance.

## G Connection between synthetic setup and natural language

### G.1 Discrete regression setup

Due to the synthetic nature of our setup, the connection to natural language is not immediately apparent. To illustrate how unobserved noise  $u$  can be interpreted linguistically, we provide a three-shot example. Each pair  $(x_j, y_j)$  can be thought of as a pair of sentences, where the second ( $y_j$ ) disambiguates the first ( $x_j$ ) for  $j \in \{1, \dots, n\}$ . In this setup,  $x_j$  is semantically ambiguous, and  $y_j$  provides a clarifying continuation. After presenting the model with  $n$  such in-context examples, we prompt it to resolve the ambiguity in a new instance, indexed by  $z$ . Figure 12 visualizes this process in natural language. The examples marked  $\diamond$ ,  $\triangle$ , and  $\square$  each consist of an ambiguous sentence  $x_j$ , followed by one or more possible concretizations  $y_j$ , with the realized continuation shown in **bold**. We then present a new ambiguous sentence  $x_z^{\text{CF}} = \textit{He was stuck in a tough spot}$ , accompanied by the index token  $\blacksquare$ . Based on the previously seen  $\square$  example, the model infers that this sentence should be interpreted in a startup context, and not related to softball/baseball or the viscoelastic polymer called *pitch*.

### G.2 Continuous SDE setup

The cyclic causal dependencies modeled by the SDEs in (3) align with the sequential structure of natural language. Each query can be interpreted as a factual narrative of length  $t_N$ . Given a hypothetical initial condition  $(x_0, y_0)$ , we task the model with counterfactually completing the story while keeping the noise fixed. This noise may represent semantic variability as well as narrative-internal uncertainty. By doing so, the model can generate plausible counterfactual continuations conditioned on the observed prompt. This approach resonates with the work of Qin et al. [2019], who explore how language models can reason about alternative story outcomes through counterfactual perturbations to character actions or events.

◇ They went to the bank.	{ There, they withdrew some money before the shops closed. They sat down and watched the ducks swim in the river. <b>After last night's storm, they had to check on the erosion.</b>
△ He broke the bat.	{ <b>The wooden handle snapped after he hit the ball too hard.</b> His little sister was very sad about the loss of her favorite stuffed toy.
□ She made a pitch.	{ The ball curved slightly as it left her hand and hit the strike zone. <b>Her voice rose as she delivered the startup idea to the investors.</b> She spread the sticky substance across the seams of the roof tiles.
■ He was stuck in a tough spot.	{ With the bases loaded and two outs, he had no room for error. <b>The product wasn't gaining traction, and investors were starting to lose interest.</b> The thick black goo clung to his boots as he tried to move across the roof.

Figure 12: **Discrete ambiguity resolution via in-context examples.** Each row shows a pair  $(x_j, y_j)$ , where  $x_j$  is an ambiguous sentence and  $y_j$  its concretization. The correct interpretation of  $y_j$  is shown in **bold**, while alternative continuations illustrate other plausible meanings of  $x_j$ . The final row (■) presents a new ambiguous sentence  $x_z^{\text{CF}}$ . Based on the prior example □, the model is expected to resolve the ambiguity in a startup context, rejecting interpretations tied to baseball or material substances.